A β-Arrestin–Biased Agonist of the Parathyroid Hormone Receptor (PTH1R) Promotes Bone Formation Independent of G Protein Activation

Diane Gesty-Palmer[1,2], **Pat Flannery**[1], **Ling Yuan**[1], **Leonor Corsino**[1], **Robert Spurney**[1], **Robert J. Lefkowitz**[1,3,4,*], and **Louis M. Luttrell**[5,6,7]

[1] Department of Medicine, Duke University Medical Center, Durham, NC 27710, USA

[2] Durham Veterans Affairs Medical Center, Durham, NC 27705, USA

[3] Department of Biochemistry, Duke University Medical Center, Durham, NC 27710, USA

[4] Howard Hughes Medical Institute, Duke University Medical Center, Durham, NC 27710, USA

[5] Department of Medicine, Medical University of South Carolina, Charleston, SC 29425, USA

[6] Department of Biochemistry and Molecular Biology, Medical University of South Carolina, Charleston, SC 29425, USA

[7] The Ralph H. Johnson Veterans Affairs Medical Center, Charleston, SC 29401, USA

Abstract

About 40% of the therapeutic agents in use today exert their effects through seven-transmembrane receptors (7TMRs). When activated by ligands, these receptors trigger two pathways that independently transduce signals to the cell: one through heterotrimeric GTP-binding proteins (G proteins) and one through β-arrestins; so-called biased agonists can selectively activate these distinct pathways. Here, we investigate selective activation of these pathways through the use of a biased agonist for the type 1 parathyroid hormone (PTH)–PTH-related protein receptor (PTH1R), (D-Trp^{12}, Tyr^{34})-PTH(7–34) (PTH-βarr), which activates β-arrestin but not classic G protein signaling. In mice, PTH-βarr induces anabolic bone formation, as does the nonselective agonist PTH (1–34), which activates both mechanisms. In β-arrestin2–null mice, the increase in bone mineral density evoked by PTH(1–34) is attenuated and that stimulated by PTH-βarr is ablated. The β-arrestin2–dependent pathway contributes primarily to trabecular bone formation and does not stimulate bone resorption. These results show that a biased agonist selective for the β-arrestin pathway can elicit a response in vivo distinct from that elicited by nonselective agonists. Ligands with these properties may form the basis for improved 7TMR-directed pharmacologic agents with enhanced therapeutic specificity.

INTRODUCTION

Parathyroid hormone (PTH), an 84–amino acid peptide hormone, is a principal regulator of calcium and phosphate homeostasis. PTH(1–34) has the biochemical and physiologic properties of the full-length PTH and is used to treat osteoporosis. Osteoblasts, which build bone, and osteoclasts, which resorb bone, are the key cellular modulators of bone remodeling and metabolism. PTH(1–34) directly stimulates osteoblasts by increasing osteoblast number and activity, promoting the deposition of new bone matrix, and accelerating the rate of mineralization. At the same time, PTH(1–34) stimulates bone resorption by increasing the recruitment, differentiation, and activity of osteoclasts—effects that are indirect. Osteoclasts lack PTH receptors but respond to factors, including receptor activator of nuclear factor κB ligand (RANKL) and osteoprotegrin (OPG), secreted by osteoblasts in response to PTH(1–34) . Because the anabolic and catabolic effects of PTH(1–34) are coupled, the net effect of PTH(1–34) on bone is dependent on the kinetics of receptor activation, with intermittent exposure leading to a net increase in bone formation, whereas continuous exposure produces net bone loss (1–3). This coupling limits the therapeutic usefulness of PTH(1–34) , because PTH(1–34) is currently administered as a daily subcutaneous injection and carries the risk of hypercalcemia (4).

The physiologic actions of PTH(1–34) have been thought to be mediated by classic heterotrimeric GTP-binding protein (G protein) signaling mechanisms (5–7). PTH(1–34) binds to the type 1 PTH–PTH-related peptide receptor (PTH1R), a seven-transmembrane receptor (7TMR) highly expressed in the kidney and bone, and activates the G_s-mediated adenylate cyclase–cAMP (adenosine 3′,5′-monophosphate)–PKA (protein kinase A) and $G_{q/11}$-mediated phospholipase C–β (PLC-β)–inositol 1,4,5-trisphosphate (IP_3)–protein kinase C (PKC) signaling pathways (8,9). Additionally, PTH(1–34) activates the RAF-MEK-ERK mitogen-activated protein kinase (MAPK) cascade through both PKA and PKC in a cell-specific and G protein–dependent manner (10–12).

7TMRs can trigger signaling mechanisms that are distinct from the classic G protein second messenger–dependent pathways. One such mechanism involves β-arrestins, a small family of cytosolic proteins initially identified for their central role in 7TMR desensitization (13–15). β-arrestins can also act as signal transducers through their formation of scaffolding complexes with accessory effector molecules such as Src, Raf, ERK1/2, JNK3 (c-Jun N-terminal kinase 3), and MAPK kinase 4 (MKK4) (16–22). PTH(1–34) stimulation of PTH1R promotes translocation of both β-arrestin1 and β-arrestin2 to the plasma membrane, association of the receptor with β-arrestins, internalization of receptor–β-arrestin complexes, and activation of ERK1/2 (11,23,24).

β-Arrestin2 influences bone remodeling and the anabolic effects of intermittent PTH(1–34) administration in mice (25,26). Ferrari *et al.* reported that intermittent administration of PTH (1–34) (80 μg/kg per day) enhanced bone mass in female β-arrestin2$^{-/-}$ knockout mice but failed to have an anabolic effect in male knockout animals. The lack of effect in the male β-arrestin2$^{-/-}$ mice was attributed to the loss of β-arrestin–mediated desensitization of G protein–coupled signaling, increased and sustained cAMP, and increased osteoclastogenesis. These findings are consistent with an increase in the G protein–coupled resorptive effect of the hormone.

We have recently shown in vitro that PTH(1–34) stimulation of the PTH1R activates ERK1/2 MAPK by two temporally distinct mechanisms: a conventional G protein–dependent pathway and a G protein–independent pathway transmitted by β-arrestins (11). Furthermore, these distinct mechanisms of MAPK activation can be selectively stimulated through the use of PTH analogs that preferentially induce G protein– or β-arrestin–coupled conformations of the

receptor. Such ligands with the ability to preferentially activate one of two distinct signaling pathways through the same receptor are referred to as biased agonists (27–31). It is not currently known whether the selective activation of β-arrestin–mediated signaling in vivo by such PTH agonists would have direct anabolic or catabolic effects on bone. All of the physiologic actions of PTH are currently ascribed to classic G protein–mediated signaling. We therefore sought to determine the consequences in vivo of β-arrestin–mediated signaling through the PTH1R on bone physiology in mice.

RESULTS

PTH-βarr stimulates β-arrestin–mediated ERK1/2 activation independent of G protein signaling

Using a previously described inverse agonist at the PTH1R, PTH-βarr [(D-Trp^{12}, Tyr^{34})-PTH (7–34)] (32), we have recently shown that PTH-βarr has the ability to stimulate β-arrestin–mediated ERK1/2 activation independent of heterotrimeric G protein activation in a transfected human embryonic kidney 293 (HEK293) cell culture system (11). To test whether PTH-βarr exhibits a similar biased response in cells that have not been engineered, we examined cAMP accumulation in response to PTH(1–34) and PTH-βarr stimulation of endogenous PTH1R in primary murine osteoblasts (POBs) (Fig. 1A). Basal cAMP concentrations in confluent, differentiated β-arrestin2$^{-/-}$ POBs were modestly, but significantly, higher than in wild-type (WT) POBs. Because β-arrestins bind active 7TMRs and uncouple them from their G protein effectors (13), the elevated basal cAMP in the knockout POBs indicates that endogenous β-arrestin2 tonically shifts the equilibrium between inactive G$_s$-coupled 7TMRs and those in the G$_s$-active state. Treatment of both WT and β-arrestin2$^{-/-}$ cells with 100 nM PTH(1–34) for 5 min generated robust increases in cAMP to an amount that did not differ significantly. Treatment of WT POBs with 1 μM PTH-βarr did not increase cAMP, whereas the same treatment of the β-arrestin2$^{-/-}$ POBs significantly lowered the elevated basal cAMP concentrations (Fig. 1A), a pattern consistent with inverse agonist activity of PTH-βarr. Thus, PTH-βarr does not promote PTH1R G$_s$ coupling in β-arrestin–replete WT POBs. Moreover, by acting as an inverse agonist, PTH-βarr diminishes G$_s$ coupling to adenylyl cyclase and reduces the low but detectable level of constitutive adenylyl cyclase activity in β-arrestin2$^{-/-}$ osteoblasts. Stimulation of POB cultures with PTH-βarr did not activate G$_{q/11}$ phosphoinositide (PI) hydrolysis (fig. S1).

PTH1R-stimulated ERK1/2 MAPK activation was assessed in WT and β-arrestin2$^{-/-}$ POBs after treatment with 100 nM PTH(1–34) or 1 μM PTH-βarr (Fig. 1B). In WT POBs, both agents increased ERK1/2 phosphorylation by about threefold. β-arrestin2$^{-/-}$ POBs showed the same response to PTH(1–34) as WT POB, indicating that the full agonist peptide can activate ERK1/2 through classic G protein–dependent pathways in the absence of β-arrestin2 (10). In contrast, PTH-βarr failed to activate ERK1/2 in β-arrestin2$^{-/-}$ POBs (Fig. 1B). Collectively, these data show that PTH-βarr, despite its inability to induce PTH1R-stimulated G protein activation, is capable of inducing PTH1R-stimulated ERK1/2 activation through a β-arrestin–dependent signaling mechanism. This qualitative reversal of efficacy is the hallmark of a biased 7TMR agonist (30,31).

β-arrestin–dependent PTH1R signaling contributes to increased bone mineral density in vivo

β-arrestin2$^{-/-}$ mice are fertile and show no gross phenotypic abnormalities (33), nor do they show gross alterations in skeletal morphology or size by x-ray analysis when compared to WT mice (fig. S2). To examine the contribution of β-arrestin–mediated signaling to the anabolic effects of PTH on bone, 9-week-old male WT and β-arrestin2$^{-/-}$ mice were treated with intermittent (once daily) intraperitoneal injection of PTH(1–34) (40 μg/kg per day), the β-arrestin–biased agonist PTH-βarr (40 μg/kg per day), or phosphate-buffered saline (PBS)

vehicle. Bone mineral density (BMD) measurements were obtained at baseline and repeated after 4 and 8 weeks of treatment (Fig. 2). At baseline, β-arrestin2$^{-/-}$ mice had significantly lower lumbar spine BMD compared to 9-week-old WT mice (WT, 0.0678 ± 0.0008 g/cm^2; β-arrestin2$^{-/-}$, 0.0648 ± 0.0009 g/cm^2; $P = 0.012$, two-tailed unpaired t test). There were no significant differences in whole-body BMD or femoral BMD between the WT and β-arrestin2$^{-/-}$ mice. As expected, at 4 and 8 weeks, WT mice treated with PTH(1–34) showed significant increases in their lumbar spine and femoral BMD compared to vehicle-treated controls, which lost BMD over the treatment period (Fig. 2, A and C). These increases in BMD were delayed in PTH(1–34) -treated β-arrestin2$^{-/-}$ mice, only reaching statistical significance in the eighth week of treatment (Fig. 2, B and D). WT mice treated with PTH-βarr (40 μg/kg per day) unexpectedly showed increased lumbar spine BMD equivalent to that produced by PTH(1–34) (Fig. 2A). Treatment with PTH-βarr did not significantly affect femoral BMD in WT animals (Fig. 2C). Administration of PTH-βarr to β-arrestin2$^{-/-}$ mice resulted in decreases in both lumbar spine and femoral BMD (Fig. 2, B and D). The anabolic effect induced by PTH-βarr in the lumbar spine of WT animals, and absent in the β-arrestin2$^{-/-}$ animals, is consistent with a β-arrestin–dependent mechanism of action. The significant decreases in BMD in β-arrestin2$^{-/-}$ mice treated with PTH-βarr are likely due to the combined inhibition of G protein–mediated signaling and the absence of a β-arrestin2–dependent contribution to bone formation. These results, taken together, suggest that PTH1R-stimulated anabolic effects in trabecular bone have discrete β-arrestin– and G protein–mediated components.

The β-arrestin pathway increases trabecular bone in vivo

To determine the effects of PTH(1–34) and PTH-βarr on bone microarchitecture, quantitative computed tomography (qCT) measurements of the lumbar spine and proximal tibia were acquired from WT and β-arrestin2$^{-/-}$ mice after 8 weeks of treatment with vehicle, PTH(1–34) , or PTH-βarr. In the lumbar spine, there was no significant difference in trabecular bone volume fraction [bone volume/total volume (BV/TV)] between vehicle-treated WT and β-arrestin2$^{-/-}$ mice (Fig. 3, A and B), although vehicle-treated β-arrestin2$^{-/-}$ mice had increased trabecular thickness (Fig. 3, A and C) and significantly lower trabecular number compared to WT mice (Fig. 3, A and D). These baseline microarchitectural differences in β-arrestin2$^{-/-}$ mice probably arise from two factors: the potentiation of G$_s$ signaling due to the loss of β-arrestin desensitization and the loss of β-arrestin2–mediated signaling.

As expected, qCT analysis of lumbar vertebrae showed that WT mice treated with daily administration of PTH(1–34) for 8 weeks had significantly increased lumbar spine trabecular BV/TV (Fig. 3, A and B), trabecular thickness (Fig. 3, A and C), and trabecular number (Fig. 3, A and D) compared to vehicle-treated animals. Unanticipated, however, were the skeletal effects of PTH-βarr in WT mice. After 8 weeks of treatment, PTH-βarr also induced significant increases in lumbar spine trabecular BV/TV (Fig. 3, A and B), trabecular thickness (Fig. 3, A and C), and trabecular number (Fig. 3, A and D) when compared to vehicle-treated animals.

To test the contributions of an independent β-arrestin–mediated signaling mechanism to trabecular bone formation, β-arrestin2$^{-/-}$ mice were also treated with PTH(1–34) and PTH-βarr. β-arrestin2$^{-/-}$ mice treated with PTH(1–34) exhibited increased trabecular BV/TV compared to vehicle-treated mice (Fig. 3, A and B). At the microarchitectural level, β-arrestin2$^{-/-}$ mice treated with PTH(1–34) had significant increases in trabecular thickness (Fig. 3, A and C) but not trabecular number (Fig. 3, A and D) compared to vehicle-treated mice.

The anabolic effects of PTH-βarr seen in the WT animals were absent in the PTH-βarr–treated β-arrestin2$^{-/-}$ mice (Fig. 3, A to D), suggesting that the effects of PTH-βarr are β-arrestin dependent. Moreover, β-arrestin2$^{-/-}$ mice treated with PTH-βarr developed significant decreases in trabecular BV/TV (Fig. 3, A and B) and trabecular thickness (Fig. 3, A and C) compared to vehicle-treated counterparts. This decrease probably reflects the loss of β-arrestin–

dependent signaling in the knockout animals in combination with the inhibition of endogenous PTH-stimulated, G protein–dependent signaling events by PTH-βarr.

Due to their skeletal morphology, the proximal tibia of mice can be considered to be more representative of the weight-bearing skeleton than the lumbar spine. Examination of this region by qCT showed effects of PTH-βarr on trabecular bone morphology similar to those seen in the lumbar spine (Fig. 3E). WT animals treated with PTH(1–34) or PTH-βarr exhibited increased trabecular BV/TV compared to vehicle-treated mice (Fig. 3, E and F). In the proximal tibia, WT mice treated with daily administration of PTH(1–34) had significantly increased trabecular thickness (Fig. 3, E and G), whereas mice treated with PTH-βarr had significantly increased trabecular number (Fig. 3, E and H) compared to vehicle-treated animals. The anabolic effects of PTH-βarr seen in the WT animals were absent in PTH-βarr–treated β-arrestin2$^{-/-}$ mice.

Cortical bone indices were examined by qCT of the midfemoral shaft. There was no significant difference in periosteal circumference between the vehicle-treated WT and β-arrestin2$^{-/-}$ mice (Fig. 3I); however, the β-arrestin2$^{-/-}$ mice had greater midshaft cortical thickness than WT mice (Fig. 3J). Compared to vehicle-treated control mice, PTH(1–34) induced increased femoral periosteal circumference and increased cortical thickness (Fig. 3, I and J) in WT but not in β-arrestin2$^{-/-}$ mice. The biased agonist PTH-βarr had no effect on these cortical indices in WT mice, whereas in the β-arrestin2$^{-/-}$ mice PTH-βarr significantly decreased periosteal circumference and cortical thickness (Fig. 3, I and J).

β-Arrestin2–mediated signaling induces histomorphometric changes

Histomorphometric analyses of lumbar spine sections were consistent with the qCT of trabecular bone morphology. Osteoblast/bone surface (OBS) was not significantly different between the vehicle-treated WT and β-arrestin2$^{-/-}$ mice (Fig. 4, A and B). However, vehicle-treated β-arrestin2$^{-/-}$ mice had greater osteoid/bone surface (OS) and osteoclast/bone surface (OCS) than vehicle-treated WT (Fig. 4, A, C, and D). This increase in OCS suggests that osteoclast activation is primarily G_s dependent and that β-arrestin2 down-regulates osteoclastogenesis in vivo, consistent with its effects on basal cAMP activity in POB (Fig. 1A).

As expected, WT mice treated with PTH(1–34) had significantly increased OBS (Fig. 4, A and B), OS (Fig. 4, A and C), and OCS (Fig. 4, A and D) compared to vehicle-treated animals. β-Arrestin2$^{-/-}$ mice treated with PTH(1–34) failed to increase OBS (Fig. 4, A and B) but did exhibit significant increases in OS compared to vehicle-treated β-arrestin2$^{-/-}$ mice (Fig. 4, A and C). PTH(1–34) was unable to further increase OCS (Fig. 4, A and D) in the β-arrestin2$^{-/-}$ mice.

WT mice treated with PTH-βarr showed increased OBS (Fig. 4, A and B) and OS (Fig. 4, A and C) compared to their vehicle-treated counterparts. These effects were absent in the β-arrestin2$^{-/-}$ mice. In contrast to PTH(1–34), PTH-βarr treatment had no effect on OCS in WT mice, suggesting that selective activation of β-arrestin signaling was not sufficient to initiate osteoclast recruitment (Fig. 4, A and D).

The finding that both PTH-βarr and PTH(1–34) increased osteoblastic activity in WT mice, whereas only PTH(1–34) increased osteoblastic activity in β-arrestin2$^{-/-}$ mice, suggests that both β-arrestin–and G protein–dependent mechanisms can promote osteoblastic bone formation. In contrast, increases in osteoclastic activity appear to be predominantly G protein dependent; baseline OCS was markedly increased in vehicle- and PTH(1–34) -treated β-arrestin2$^{-/-}$ mice, where G_s signaling is unrestrained, and treatment with PTH-βarr, which inhibits PTH1R-dependent cAMP production, dramatically reduces osteoclast surface in β-arrestin2$^{-/-}$ mice (Fig. 4, A and D).

Dynamic indices of bone formation determined by calcein double labeling showed significant increases in the mineral-apposition rate and the bone-formation rate in WT mice treated with PTH(1–34) or PTH-βarr compared to vehicle-treated mice (Fig. 4, E to G). Consistent with anabolic bone formation produced by selective activation of β-arrestin–mediated signaling, PTH-βarr had no effect in the β-arrestin2$^{-/-}$ mice.

β-Arrestin–mediated signaling influences bone metabolism

Serum and 24-hour urine samples were obtained from WT and β-arrestin2$^{-/-}$ mice treated with vehicle, PTH(1–34) , or PTH-βarr. PTH (1–34), but not PTH-βarr, significantly increased 24-hour urinary calcium concentration in WT mice (fig. S3). Because PTH effects on renal calcium handling are cAMP dependent, these results are consistent with the in vitro data with POB (Fig. 1A) and confirm that PTH-βarr does not increase PTH1R-G$_s$ signaling in vivo at the doses used.

Serum osteocalcin, a biochemical marker of bone formation, was not significantly different between vehicle-treated WT and β-arrestin2$^{-/-}$ animals. PTH(1–34) or PTH-βarr treatment significantly increased osteocalcin in WT mice compared to vehicle-treated mice (Fig. 5A), and PTH(1–34) increased osteocalcin in the β-arrestin2$^{-/-}$ mice. However, PTH-βarr had no significant effect on serum osteocalcin in the β-arrestin2$^{-/-}$ mice (Fig. 5B). These data are consistent with the histomorphometric analysis of osteoblast and osteoid surface (Fig. 4, A to C) and further support the hypothesis that the anabolic effects of PTH-βarr on bone are β-arrestin dependent. Because PTH(1–34) increased serum osteocalcin in β-arrestin2$^{-/-}$ mice, it is clear that multiple PTH1R-stimulated pathways can increase osteocalcin production, both G$_s$ dependent and mediated by β-arrestins, but independent of G$_s$ activation.

After 4 weeks, vehicle-treated β-arrestin2$^{-/-}$ mice had significantly higher urine deoxypyridinoline (DPD), a marker of bone resorption, than did their vehicle-treated WT counterparts (WT, 30.78 ± 2.71 nM; β-arrestin2$^{-/-}$, 37.56 ± 2.17 nM; $P = 0.038$, two-tailed unpaired t test). This result correlates with the increase in baseline osteoclast surface determined histologically (Fig. 4, A and D) and indicates that endogenous β-arrestin2 attenuates osteoclastic bone turnover in vivo, probably by inhibiting G$_s$-dependent osteoclast formation. PTH(1–34) significantly increased urine DPD in both WT and β-arrestin2$^{-/-}$ mice compared to that in vehicle-treated animals (Fig. 5, C and D). Consistent with the lack of osteoclast recruitment histologically, PTH-βarr treatment had no significant effect on urine DPD in either WT or β-arrestin2$^{-/-}$ mice compared to vehicle treatment (Fig. 5, C and D). In addition, the increase in urine DPD excretion in the PTH(1–34) -treated β-arrestin2$^{-/-}$ mice compared to WT further supports the notion that osteoclast-mediated bone resorption is meditated through G protein–dependent mechanisms.

Distinct PTH receptor pathways regulate gene expression of bone regulatory proteins

To determine the contribution of β-arrestin2–mediated signaling to PTH1R-stimulated transcription of bone regulatory proteins, calvarial RNA was isolated from WT and β-arrestin2$^{-/-}$ mice treated with PTH (1–34), PTH-βarr, or vehicle. Gene expression for osteocalcin and for RANKL and OPG, which activate and inhibit osteoclastic bone resorption, respectively (34), was analyzed by quantitative reverse transcription–polymerase chain reaction (RT-PCR) (Fig. 6, A to C).

In vehicle-treated animals, the expression of osteocalcin was higher in β-arrestin2$^{-/-}$ mice compared to that in WT mice. Both PTH(1–34) and PTH-βarr increased in vivo expression of osteocalcin in WT-treated animals compared to that in their vehicle-treated counterparts (Fig. 6A), consistent with the qCT and histomorphometric indices of bone formation. PTH(1–34)

treatment also significantly increased the osteocalcin expression in the β-arrestin2$^{-/-}$ mice, whereas PTH-βarr treatment decreased osteocalcin expression.

The expression of the modulators of osteoclast activity, RANKL and OPG, was higher in vehicle-treated β-arrestin2$^{-/-}$ mice compared to the expression in WT mice. The increased RANKL expression is consistent with the significantly higher urine DPD in the vehicle-treated β-arrestin2$^{-/-}$ mice compared to that in WT mice. Only PTH(1–34) increased in vivo expression of RANKL and OPG in WT-treated animals compared to that in their vehicle-treated counterparts (Fig. 6, B and C). Neither PTH nor PTH-βarr treatment had a significant effect on the RANKL or OPG expression in the β-arrestin2$^{-/-}$ mice. The failure of PTH(1–34) to increase in RANKL expression in the β-arrestin2$^{-/-}$ mice is not unexpected. This finding is consistent with the histomorphometric data showing that the OCS is greater in the β-arrestin2$^{-/-}$ mice than in the WT mice. PTH(1–34) does not significantly increase OCS in the β-arrestin2$^{-/-}$–treated mice (Fig. 4D).

DISCUSSION

We have previously shown in vitro that PTH(1–34) stimulation of the PTH1R activates ERK1/2 MAPK by two temporally distinct mechanisms: one G protein dependent and the other β-arrestin dependent. Furthermore, these distinct mechanisms of MAPK activation can be selectively stimulated through the use of biased PTH agonists (11). Here, we demonstrate, using the β-arrestin pathway–selective PTH analog, PTH-βarr, that activation of β-arrestin signaling in bone is sufficient to elicit an anabolic response characterized by increased osteoblastic bone formation in the absence of detectable bone resorption.

Although PTH-mediated signals are important in bone remodeling, our findings indicate that our understanding of the mechanistic basis for PTH action is incomplete. Our results identify a role of β-arrestins in the regulation of bone formation and turnover. Mice without β-arrestin2 lack both β-arrestin2–dependent desensitization of PTH-stimulated G protein activity and β-arrestin2–mediated signaling. Despite the impaired G protein–coupled receptor desensitization, the knockout mice have normal serum calcium concentrations (35) and exhibit grossly normal skeletal structure. Circulating amounts of endogenous PTH are suppressed in the knockout animals (35), presumably a compensation for the increased sensitivity to endogenous PTH-stimulated G protein activation that permits them to maintain physiologic homeostasis. Nonetheless, genetic ablation of β-arrestin2 leads to altered PTH1R-stimulated bone metabolism, as indicated by our data. Compared to WT mice, β-arrestin2$^{-/-}$ mice exhibit significantly higher basal rates of bone turnover. Osteoid surface and osteocalcin messenger RNA (mRNA) expression is increased, consistent with an overall increase in the rate of bone formation. At the same time, osteoclast surface and bone turnover markers, such as RANKL and OPG mRNA and urine DPD, are also increased. Although their trabecular BMDs and bone volume are comparable, the knockout mice show microarchitectural differences, such as increased trabecular thickness and decreased trabecular number, likely representing the net effect of increased bone formation offset by accelerated bone resorption.

Exposure of both groups of animals to PTH(1–34) allows separation of the effects of G protein signaling from β-arrestin signaling because PTH(1–34) activates both pathways in WT animals, but only G protein signaling in the knockout animals. In WT animals, PTH(1–34) produces the expected increases in indices of bone formation: increased osteoblast number and osteoid surface and increased osteocalcin mRNA and serum osteocalcin. It also produces expected increases in osteoclastic bone resorption, as evidenced by increases in RANKL mRNA expression, osteoclast number, and urine DPD. These effects reflect the coupling of osteoblastic bone formation with osteoclastic bone resorption that occurs as a result of the production of osteoclast-activating factors, such as RANKL, by osteoblasts upon exposure to

PTH(1–34) . The net effect is increased bone formation at trabecular and cortical bone sites. In contrast, β-arrestin2$^{-/-}$ animals treated with PTH(1–34) exhibit reduced bone accrual in the lumbar spine and an absence of an increase in cortical bone compared to vehicle-treated animals. This attenuated overall response is associated with an exaggerated increase in osteoclast number and urine DPD, indicative of accelerated bone resorption.

These data are subject to two interpretations that are not mutually exclusive. Either loss of β-arrestin2 leads to exaggerated G protein signaling that stimulates greater osteoclastic bone resorption compared to osteoblastic bone formation, or it causes the loss of β-arrestin2–mediated signals required for an optimal response to PTH(1–34) , or both. The relative contributions of these two processes cannot be distinguished with β-arrestin2$^{-/-}$ animals because both functions of β-arrestin are absent and cannot be independently reconstituted. However, treating WT animals with the biased agonist PTH-βarr, which activates the β-arrestin2 pathway without increasing G protein activity, allowed us to determine whether β-arrestin–mediated signaling is sufficient to modulate osteoblast activity. We found that WT animals treated with PTH-βarr exhibit an increase in bone formation, as shown by increases in bone volume, trabecular number and thickness, osteoblast number, osteocalcin mRNA expression, and serum osteocalcin. These anabolic effects appear confined to trabecular bone. Unlike the effect of PTH(1–34) , selective activation of the β-arrestin2 pathway by PTH-βarr does not significantly increase any indices of osteoclastic bone resorption, including osteoclast number, RANKL mRNA, and urine DPD. These data suggest that a biased agonist, such as PTH-βarr, which stimulates β-arrestin2–dependent signaling without causing G protein activation, is sufficient to promote bone formation but does not simultaneously activate bone resorption. The conclusion that the net anabolic effect of PTH-βarr is dependent on β-arrestin2 is supported by our finding that all indices of bone formation and resorption either fall or remain unchanged in β-arrestin2$^{-/-}$ animals treated with PTH-βarr. In sum, these data suggest that a biased agonist that engages the PTH1R to activate β-arrestin signaling in the absence of G protein signaling promotes osteoblastic bone formation without stimulating bone resorption and may have clinical utility as an anabolic agent in the treatment of diseases characterized by insufficient rates of bone formation, such as osteoporosis.

MATERIALS AND METHODS

Materials

Human PTH(1–34) and bovine PTH-βarr were obtained from Bachem (Philadelphia, PA). Antibody against phospho-p44/42 MAPK (1:2000) was from Cell Signaling (Beverly, MA) and antibody against MAPK1/2 (1:10,000) was from Upstate Technology (Lake Placid, NY). All PCR primers were prepared by Operon Technologies (Alameda, CA).

Animals and PTH treatment

The derivation of β-arrestin2$^{-/-}$ mice was previously described (33). Mice were backcrossed for more than nine generations onto a C57BL/6J background. Mice were maintained under standard nonbarrier conditions, fed rodent chow (LabDiet, PMI Nutrition International, St. Louis, MO), and had access to water ad libitum. Human PTH(1–34) (40 μg/kg per day), bovine PTH-βarr (40 μg/kg per day), or PBS vehicle was administered to 9-week-old male mice via intraperitoneal injection daily for 8 weeks. Animal protocols were approved by the institutional animal care and use committee at Duke University School of Medicine and were in accordance with the National Institutes of Health *Guide for the Care and Use of Laboratory Animals*.

Isolation of primary osteoblasts

Primary osteoblasts were isolated from the calvaria of 8-day-old β-arrestin2$^{-/-}$ and WT C57BL/6 mice with established procedures (36). Calvaria underwent sequential digestion in 0.05%

trypsin and 0.1% collagenase at 37°C. Primary osteoblast cultures were grown to confluence and differentiated for 10 days in the presence of α-MEM supplemented with 10% fetal bovine serum and 5 mM β-glycerophosphate.

cAMP determination

PTH-stimulated cAMP was determined in primary osteoblasts isolated from β-arrestin2$^{-/-}$ and WT mice. Osteoblasts were preincubated for 15 min in α-MEM supplemented with 10 mM Hepes (pH 7.4) and 1 mM isobutylmethylxanthine and stimulated for 15 min with PTH(1–34) or PTH-βarr. Forskolin (10 μM) was used as a positive control. The stimulation was terminated with the addition of 0.125 M EDTA, and the samples were boiled for 10 min and clarified by centrifugation for 1 min at 15,000*g*. cAMP concentrations were determined with a ^{3}H-labeled cAMP assay as described (37).

Inositol phosphate determination

Osteoblasts were plated onto poly-D-lysine–coated 12-well tissue culture plates (BD Biosciences Labware) and then differentiated for 10 days before study. After differentiation, cells were equilibrated for 24 hours in labeling medium containing *myo*-[^{3}H]inositol (1 μCi/ml). Cells were washed once with PBS for 30 min at 37°C, washed with PBS containing 20 mM LiCl for 20 min at 37°C, and then treated with agonist for 20 min. Total inositol phosphates were extracted and separated as described (38).

ERK1/2 assay

ERK1/2 activation was assessed in primary osteoblasts isolated from β-arrestin2$^{-/-}$ and WT mice. Primary osteoblasts were starved for 12 to 18 hours in serum-free medium before stimulation with 100 nM PTH(1–34) or 1 μM PTH-βarr for 5 min. After stimulation, medium was removed and 100 μl of 2× Laemmli sample buffer was added to each well. Immunoblotting and chemiluminescent detection were performed as described with Pico ECL (Amersham) (11).

Radiography, bone densitometry, and qCT

Radiography of mice was performed with a Faxitron 43807N series Radiograph System (Faxitron X-Ray Corp., Wheeling, IL). BMD of murine lumbar spine and femurs was assessed with a Lunar PIXImus bone densitometer (Lunar Corp., Madison, WI) as previously described (39). High-resolution qCT (μCT40; Scanco Medical, Bassersdorf, Switzerland) was used to evaluate trabecular bone volume fraction and microarchitecture in the lumbar vertebral spine and proximal tibia and cortical bone geometry. For examination of the vertebral spine, the volume of interest included the entire trabecular region within the vertebral body. Trabecular morphometric analysis was performed on four lumbar vertebrae per animal. Cortical bone parameters were determined on the midfemoral shaft. Samples were scanned at 45 keV with cone beam mode and a slice increment of 6 μm. Images from each group were generated at 275 threshold. The three-dimensional volume of interest structure was constructed and analyzed with the internal software of the μCT system.

Histomorphometry

Quantitative histomorphometric analysis of vertebral spine trabecular bone was performed with techniques described previously (40). Mice were given an intraperitoneal injection of calcein (15 μg of calcein per gram of body weight) on days 3 and 10 before being killed. After harvesting, nondecalcified sections were fixed in 70% ethanol, stained with Villanueva stain, embedded in methyl methacrylate, and sectioned longitudinally at a thickness of 5 to 10 μm with a Polycut E microtome (Leica Corp. Microsystems AG, Glattbrugg, Switzerland). The 5-μm sections were stained with Goldner's stain and analyzed under transmitted light, and the

10-μm Villanueva prestained sections were analyzed under fluorescent light with previously described methods (36). Images were acquired with a Provis AX70 microscope (Olympus, Tokyo, Japan) equipped with a Spot RT digital camera and processed with Image-Pro Plus and Adobe Photoshop. Primary measurements were directly obtained by superimposing a graticule identifying a minimum of 100 bone surface intersections on a minimum of three fields from three sections. Mineral apposition rates and bone formation rates were determined from calcein double labeling. Calcein double-labeling distance was measured directly with microscope imaging software. Magnification varied from 40× to 100× for two-point analyses and cell counting. The terminology and units used are those recommended by the histomorphometry nomenclature committee of the American Society of Bone and Mineral Research (41).

Serum biochemistry and bone turnover markers

Blood was collected retroorbitally or by cardiac puncture. Serum osteocalcin concentrations were quantitated with a two-site immunoradiometric assay from Immunotopics (San Clemente, CA) according to the directions of the manufacturer. Urine was collected for 24 hours from mice housed in metabolic cages (Hatteras Instruments, Hatteras, NC). DPD excretion was quantitated with the Pyrilinks-D assay kit (Metra Biosystems, Mountain View, CA). Urine creatinine concentration was measured by the Jaffé alkaline picrate method with a kit from Exocell (Philadelphia, PA). Urine ionized calcium measurements were obtained with a micro mono calcium ion electrode (Lazar Research Laboratories, Los Angeles, CA).

Calvarial gene expression

Total cellular RNA was isolated from the calvaria of the animals treated for 8 weeks with vehicle, PTH(1–34) , or PTH-βarr. The RNA was isolated by previously described standard methods (39). Tissue samples were thawed in TRIzol reagent (Invitrogen, Carlsbad, CA) and homogenized. RNA extraction was performed according to the TRIzol manufacturer's protocol. Reverse transcription reactions were performed with the iScript cDNA Synthesis kit (Bio-Rad). Real-time quantitative PCR was performed with the iCycler iQ Real-Time PCR Detection System (Bio-Rad) and Universal SYBR Green PCR Master Mix kit (Bio-Rad).

Statistics

All values are expressed as means ± SEM. For comparisons between two groups, statistical significance was assessed with a two-tailed unpaired t test. One-way analysis of variance (ANOVA) with Bonferroni multiple comparisons post test was used to assess the effect of PTH and PTH-βarr on WT and β-arrestin2$^{-/-}$ skeletal morphology. The computations and graphs were performed and constructed with the GraphPad Prism 4.0 scientific graphing, curve fitting, and statistics program (GraphPad Software, San Diego, CA).

Supplementary Material

Refer to Web version on PubMed Central for supplementary material.

Acknowledgments

REFERENCES AND NOTES

1. Qin L, Raggatt LJ, Partridge NC. Parathyroid hormone: A double-edged sword for bone metabolism. Trends Endocrinol Metab 2004;15:60–65. [PubMed: 15036251]

2. Hock JM, Gera I. Effects of continuous and intermittent administration and inhibition of resorption on the anabolic response of bone to parathyroid hormone. J Bone Miner Res 1992;7:65–72. [PubMed: 1532281]

3. Dobnig H, Turner RT. Evidence that intermittent treatment with parathyroid hormone increases bone formation in adult rats by activation of bone lining cells. Endocrinology 1995;136:3632–3638. [PubMed: 7628403]

4. Girotra M, Rubin MR, Bilezikian JP. The use of parathyroid hormone in the treatment of osteoporosis. Rev Endocr Metab Disord 2006;7:113–121. [PubMed: 17043762]

5. Koh AJ, Beecher CA, Rosol TJ, McCauley LK. 3′,5′-Cyclic adenosine monophosphate activation in osteoblastic cells: Effects on parathyroid hormone-1 receptors and osteoblastic differentiation in vitro. Endocrinology 1999;140:3154–3162. [PubMed: 10385409]

6. Ishizuya T, Yokose S, Hori M, Noda T, Suda T, Yoshiki S, Yamaguchi A. Parathyroid hormone exerts disparate effects on osteoblast differentiation depending on exposure time in rat osteoblastic cells. J Clin Invest 1997;99:2961–2970. [PubMed: 9185520]

7. Hilliker S, Wergedal JE, Gruber HE, Bettica P, Baylink DJ. Truncation of the amino terminus of PTH alters its anabolic activity on bone in vivo. Bone 1996;19:469–477. [PubMed: 8922645]

8. Bringhurst FR, Juppner H, Guo J, Urena P, Potts JT Jr, Kronenberg HM, Abou-Samra AB, Segre GV. Cloned, stably expressed parathyroid hormone (PTH)/PTH-related peptide receptors activate multiple messenger signals and biological responses in LLC-PK1 kidney cells. Endocrinology 1993;132:2090–2098. [PubMed: 8386606]

9. Swarthout JT, D'Alonzo RC, Selvamurugan N, Partridge NC. Parathyroid hormone-dependent signaling pathways regulating genes in bone cells. Gene 2002;282:1–17. [PubMed: 11814673]

10. Cole JA. Parathyroid hormone activates mitogen-activated protein kinase in opossum kidney cells. Endocrinology 1999;140:5771–5779. [PubMed: 10579343]

11. Gesty-Palmer D, Chen M, Reiter E, Ahn S, Nelson CD, Wang S, Eckhardt AE, Cowan CL, Spurney RF, Luttrell LM, Lefkowitz RJ. Distinct β-arrestin- and G protein-dependent pathways for parathyroid hormone receptor-stimulated ERK1/2 activation. J Biol Chem 2006;281:10856–10864. [PubMed: 16492667]

12. Verheijen MH, Defize LH. Parathyroid hormone activates mitogen-activated protein kinase via a cAMP-mediated pathway independent of Ras. J Biol Chem 1997;272:3423–3429. [PubMed: 9013586]

13. Luttrell LM, Lefkowitz RJ. The role of β-arrestins in the termination and transduction of G-protein-coupled receptor signals. J Cell Sci 2002;115:455–465. [PubMed: 11861753]

14. Freedman NJ, Lefkowitz RJ. Desensitization of G protein-coupled receptors. Recent Prog Horm Res 1996;51:319–351. discussion 352–353. [PubMed: 8701085]

15. Pierce KL, Lefkowitz RJ. Classical and new roles of β-arrestins in the regulation of G-protein-coupled receptors. Nat Rev Neurosci 2001;2:727–733. [PubMed: 11584310]

16. Luttrell LM, Ferguson SS, Daaka Y, Miller WE, Maudsley S, Della Rocca GJ, Lin F, Kawakatsu H, Owada K, Luttrell DK, Caron MG, Lefkowitz RJ. β-arrestin-dependent formation of β2 adrenergic receptor-Src protein kinase complexes. Science 1999;283:655–661. [PubMed: 9924018]

17. Shenoy SK, Lefkowitz RJ. Seven-transmembrane receptor signaling through β-arrestin. Sci STKE 2005 2005:cm10.

18. Lefkowitz RJ, Shenoy SK. Transduction of receptor signals by β-arrestins. Science 2005;308:512–517. [PubMed: 15845844]

19. DeWire SM, Ahn S, Lefkowitz RJ, Shenoy SK. β-arrestins and cell signaling. Annu Rev Physiol 2007;69:483–510. [PubMed: 17305471]

20. McDonald PH, Chow CW, Miller WE, Laporte SA, Field ME, Lin FT, Davis RJ, Lefkowitz RJ. β-arrestin 2: A receptor-regulated MAPK scaffold for the activation of JNK3. Science 2000;290:1574–1577. [PubMed: 11090355]

21. DeFea KA, Zalevsky J, Thoma MS, Dery O, Mullins RD, Bunnett NW. β-arrestin-dependent endocytosis of proteinase-activated receptor 2 is required for intracellular targeting of activated ERK1/2. J Cell Biol 2000;148:1267–1281. [PubMed: 10725339]

22. Luttrell LM, Roudabush FL, Choy EW, Miller WE, Field ME, Pierce KL, Lefkowitz RJ. Activation and targeting of extracellular signal-regulated kinases by β-arrestin scaffolds. Proc Natl Acad Sci USA 2001;98:2449–2454. [PubMed: 11226259]

23. Ferrari SL, Behar V, Chorev M, Rosenblatt M, Bisello A. Endocytosis of ligand-human parathyroid hormone receptor 1 complexes is protein kinase C-dependent and involves β-arrestin2. Real-time monitoring by fluorescence microscopy. J Biol Chem 1999;274:29968–29975. [PubMed: 10514480]

24. Vilardaga JP, Krasel C, Chauvin S, Bambino T, Lohse MJ, Nissenson RA. Internalization determinants of the parathyroid hormone receptor differentially regulate β-arrestin/receptor association. J Biol Chem 2002;277:8121–8129. [PubMed: 11726668]

25. Bouxsein ML, Pierroz DD, Glatt V, Goddard DS, Cavat F, Rizzoli R, Ferrari SL. β-Arrestin2 regulates the differential response of cortical and trabecular bone to intermittent PTH in female mice. J Bone Miner Res 2005;20:635–643. [PubMed: 15765183]

26. Ferrari SL, Pierroz DD, Glatt V, Goddard DS, Bianchi EN, Lin FT, Manen D, Bouxsein ML. Bone response to intermittent parathyroid hormone is altered in mice null for β-arrestin2. Endocrinology 2005;146:1854–1862. [PubMed: 15705780]

27. Kenakin T. Inverse, protean, and ligand-selective agonism: Matters of receptor conformation. FASEB J 2001;15:598–611. [PubMed: 11259378]

28. Brzostowski JA, Kimmel AR. Signaling at zero G: G-protein-independent functions for 7-TM receptors. Trends Biochem Sci 2001;26:291–297. [PubMed: 11343921]

29. Kenakin T. Functional selectivity through protean and biased agonism: Who steers the ship? Mol Pharmacol 2007;72:1393–1401. [PubMed: 17901198]

30. Gesty-Palmer D, Luttrell LM. Heptahelical terpsichory. Who calls the tune? J Recept Signal Transduct Res 2008;28:39–58. [PubMed: 18437629]

31. Violin JD, Lefkowitz RJ. β-arrestin-biased ligands at seven-transmembrane receptors. Trends Pharmacol Sci 2007;28:416–422. [PubMed: 17644195]

32. Gardella TJ, Luck MD, Jensen GS, Schipani E, Potts JT Jr, Jüppner H. Inverse agonism of amino-terminally truncated parathyroid hormone (PTH) and PTH-related peptide (PTHrP) analogs revealed with constitutively active mutant PTH/PTHrP receptors. Endocrinology 1996;137:3936–3941. [PubMed: 8756569]

33. Bohn LM, Lefkowitz RJ, Gainetdinov RR, Peppel K, Caron MG, Lin FT. Enhanced morphine analgesia in mice lacking β-arrestin 2. Science 1999;286:2495–2498. [PubMed: 10617462]

34. Hofbauer LC, Schoppet M. Clinical implications of the osteoprotegerin/RANKL/RANK system for bone and vascular diseases. JAMA 2004;292:490–495. [PubMed: 15280347]

35. Pi M, Oakley RH, Gesty-Palmer D, Cruickshank RD, Spurney RF, Luttrell LM, Quarles LD. β-arrestin- and G protein receptor kinase-mediated calcium-sensing receptor desensitization. Mol Endocrinol 2005;19:1078–1087. [PubMed: 15637145]

36. Garner SC, Pi M, Tu Q, Quarles LD. Rickets in cation-sensing receptor-deficient mice: An unexpected skeletal phenotype. Endocrinology 2001;142:3996–4005. [PubMed: 11517179]

37. Zamah AM, Delahunty M, Luttrell LM, Lefkowitz RJ. Protein kinase A-mediated phosphorylation of the β_2-adrenergic receptor regulates its coupling to G_s and G_i. Demonstration in a reconstituted system. J Biol Chem 2002;277:31249–31256. [PubMed: 12063255]

38. Cotecchia S, Ostrowski J, Kjelsberg MA, Caron MG, Lefkowitz RJ. Discrete amino acid sequences of the α_1-adrenergic receptor determine the selectivity of coupling to phosphatidylinositol hydrolysis. J Biol Chem 1992;267:1633–1639. [PubMed: 1309789]

39. Wang L, Liu S, Quarles LD, Spurney RF. Targeted overexpression of G protein-coupled receptor kinase-2 in osteoblasts promotes bone loss. Am J Physiol Endocrinol Metab 2005;288:E826–E834. [PubMed: 15585587]

40. Spurney RF, Flannery PJ, Garner SC, Athirakul K, Liu S, Guilak F, Quarles LD. Anabolic effects of a G protein-coupled receptor kinase inhibitor expressed in osteoblasts. J Clin Invest 2002;109:1361–1371. [PubMed: 12021252]

41. Parfitt AM, Drezner MK, Glorieux FH, Kanis JA, Malluche H, Meunier PJ, Ott SM, Recker RR. Bone histomorphometry: Standardization of nomenclature, symbols, and units. Report of the ASBMR Histomorphometry Nomenclature Committee. J Bone Miner Res 1987;2:595–610. [PubMed: 3455637]
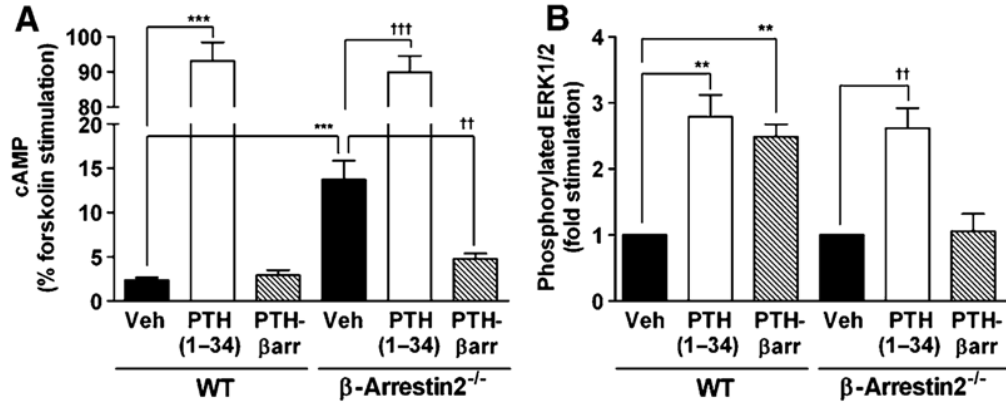
Fig. 1.
PTH-βarr stimulates β-arrestin–mediated ERK1/2 activation, independent of G protein signaling, in osteoblasts. (**A**) cAMP activation in response to PTH(1–34) and PTH-βarr stimulation of endogenously expressed PTH1R in POBs isolated from β-arrestin2$^{-/-}$ and WT C57BL/6 mice. cAMP values were normalized to 10 μM forskolin–induced concentrations (2.24 ± 0.2 μM). Data correspond to the mean ± SEM from four independent experiments. ***$P < 0.001$ compared with the vehicle-stimulated WT POBs. $^{†††}P < 0.001$; $^{††}P < 0.01$ compared with the vehicle-stimulated β-arrestin2$^{-/-}$ POBs; direct comparisons were made with two-tailed unpaired t test. Veh, vehicle. (**B**) PTH(1–34) and PTH-βarr stimulated ERK1/2 activation in POBs isolated from β-arrestin2$^{-/-}$ and WT C57BL/6 mice. Values presented are the fold ERK1/2 phosphorylation over vehicle-stimulated controls. Data represent the mean ± SEM from four independent experiments. **$P < 0.01$ compared with the vehicle-stimulated WT POBs. $^{††}P < 0.01$ compared with the vehicle-stimulated β-arrestin2$^{-/-}$ POBs; direct comparisons were made with two-tailed unpaired t test.
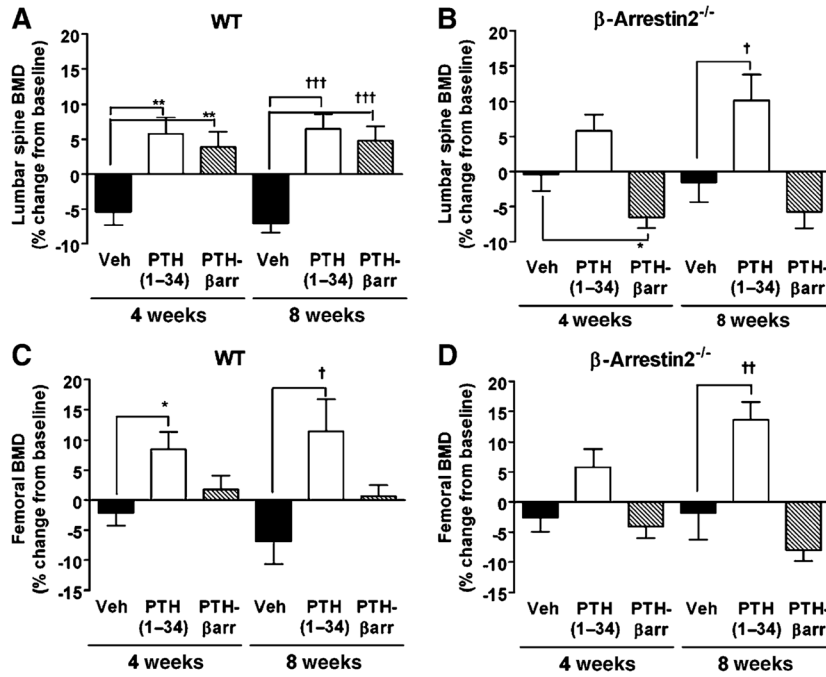
Fig. 2.
PTH-βarr increases lumbar spine BMD. (**A** and **B**) Lumbar spine and (**C** and **D**) femoral BMD of male WT and β-arrestin2$^{-/-}$ mice treated with vehicle (Veh), 1-34), or PTH-βarr was determined by dual-energy x-ray absorption. Mice were treated starting at 9 weeks of age. Data represent the mean percent change from baseline BMD ± SEM of measurements taken from at least seven male mice. *$P < 0.05$; **$P < 0.01$ compared with vehicle-treated WT mice. $^{\dagger}P < 0.05$, $^{\dagger\dagger}P < 0.01$, $^{\dagger\dagger\dagger}P < 0.001$ compared with vehicle-treated β-arrestin2$^{-/-}$ mice; significance was determined with one-way ANOVA with Bonferroni multiple comparisons post test.
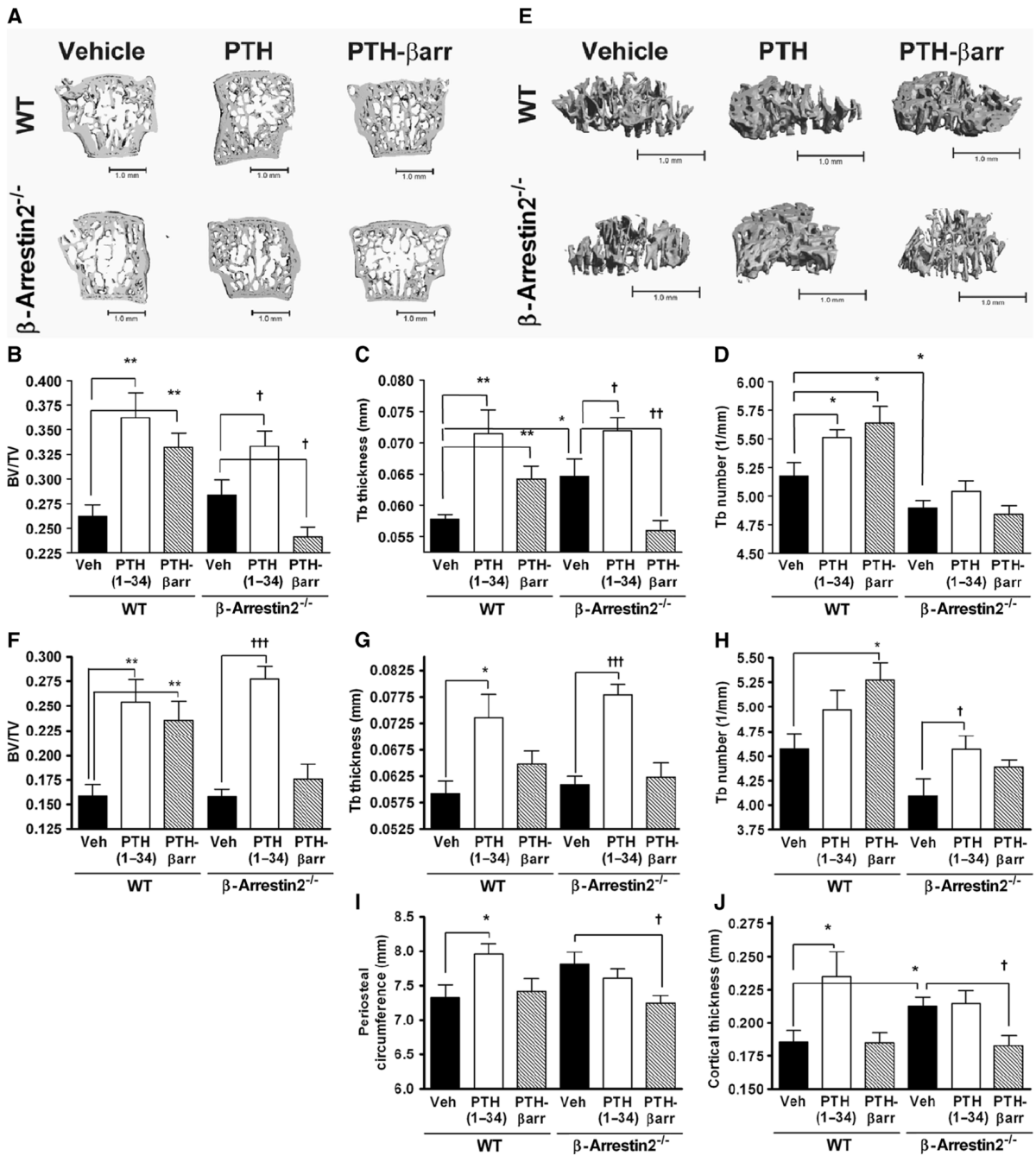
Fig. 3.
β-Arrestin2–dependent signaling contributes to increases in trabecular but not cortical bone.
(**A**) Representative qCT of lumbar vertebrae isolated from male WT and β-arrestin2$^{-/-}$ mice
treated for 8 weeks with vehicle, PTH(1–34), or PTH-βarr. Scale bar, 1.0 mm. Mice were
treated starting at 9 weeks of age. qCT of the lumbar spine was used to determine the effects
on (**B**) trabecular bone (Tb) volume fraction (BV/TV), (**C**) Tb thickness, and (**D**) Tb number.
(**E**) Representative qCT of proximal tibia from male WT and β-arrestin2$^{-/-}$ mice treated for 8
weeks with vehicle, PTH(1–34), or PTH-βarr. Scale bar, 1.0 mm. qCT of proximal tibia was
used to determine the effects on (**F**) Tb volume fraction (BV/TV), (**G**) Tb thickness, and (**H**)
Tb number. qCT of the mid-femoral shaft was used to determine (**I**) periosteal circumference

and (**J**) cortical thickness. Data represent the mean ± SEM of measurements taken from at least seven male mice. *$P < 0.05$; **$P < 0.01$; ***$P < 0.001$ compared with vehicle-treated WT mice. †$P < 0.05$; ††$P < 0.01$; †††$P < 0.001$ compared with vehicle-treated β-arrestin2$^{-/-}$ mice; significance was determined with one-way ANOVA with Bonferroni multiple comparisons post test.
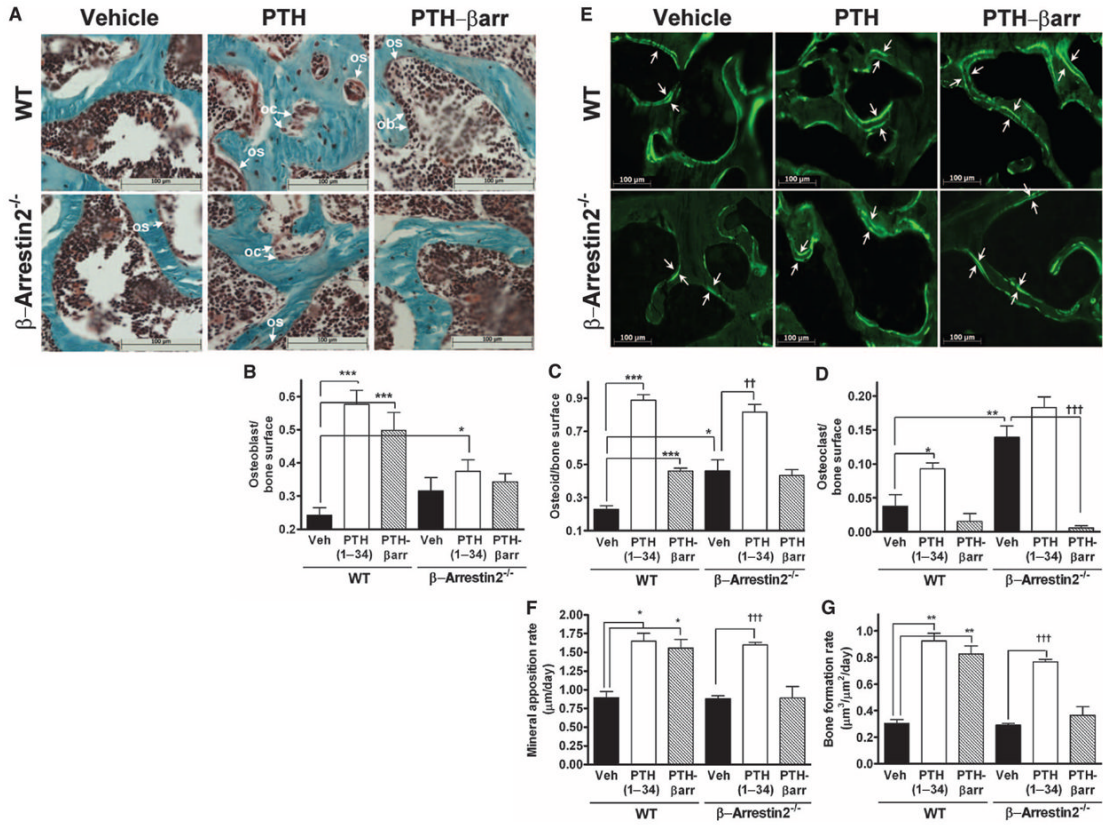
Fig. 4.
Bone histomorphometry and dynamic indices of bone formation in WT and β-arrestin2^{−/−} mice.
(**A**) Representative nondecalcified, 5-μm sections of lumbar vertebrae isolated from male WT
and β-arrestin2^{−/−} mice treated at 9 weeks of age for 8 weeks with vehicle, PTH(1–34), or
PTH-βarr. Scale bar, 100 μm. ob, osteoblasts; oc, osteoclasts; os, osteoid. Quantitated
histomorphometric analysis of (**B**) OBS, (**C**) OS, and (**D**) OCS after treatment with either
vehicle, PTH(1–34), or PTH-βarr. Data represent the mean ± SEM of measurements from four
mice. (**E**) Representative calcein double-labeled, nondecalcified, 10-μm sections of lumbar
vertebrae isolated from male WT and β-arrestin2^{−/−} mice treated for 8 weeks with either
vehicle, PTH, or PTH-βarr. Scale bar, 100 μm. Bone growth is determined by measuring the
distance between calcein-labeled layers (arrows). Quantitation of the (**F**) mineral apposition
rate and (**G**) bone formation rates from calcein-labeled trabecular bone. Data represent the
mean ± SEM of measurements from four mice. *$P < 0.05$; **$P < 0.01$; ***$P < 0.001$ compared
with vehicle-treated mice. [†]$P < 0.05$; [††]$P < 0.01$; [†††]$P < 0.001$ compared with vehicle-treated
β-arrestin2^{−/−} mice; significance determined with one-way ANOVA with Bonferroni
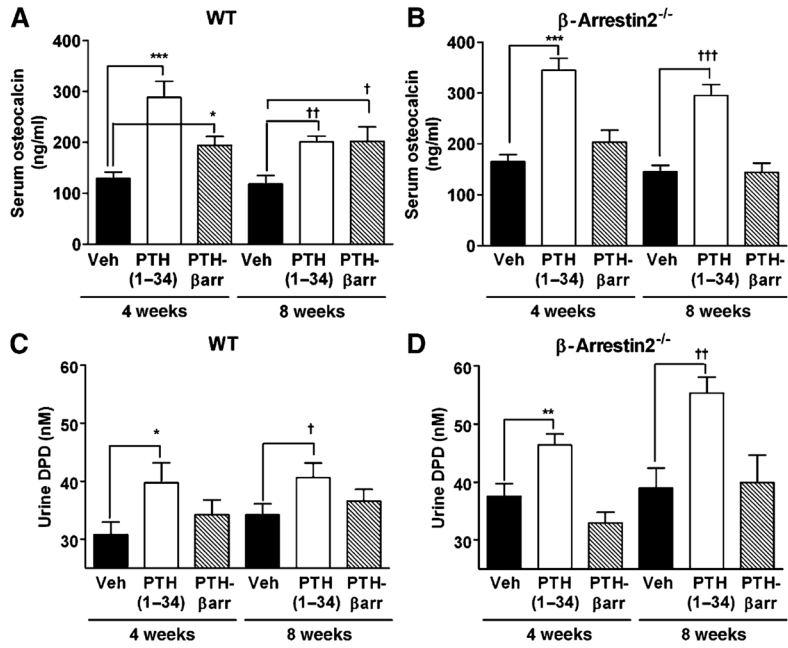correction.

Fig. 5.
PTH-βarr increases serum osteocalcin but has no effect on urine DPD excretion. Osteocalcin was measured in serum obtained from male (**A**) WT and (**B**) β-arrestin2$^{-/-}$ mice after 4 and 8 weeks of treatment with vehicle, PTH(1–34), or PTH-βarr. Twenty-four-hour urine DPD was measured in male (**C**) WT and (**D**) β-arrestin2$^{-/-}$ mice after 4 and 8 weeks of treatment with vehicle, PTH(1–34), or PTH-βarr. Mice were treated starting at 9 weeks of age. Data represent the mean ± SEM of measurements taken from at least seven male mice. *$P < 0.05$; **$P < 0.01$; ***$P < 0.001$ compared with vehicle-treated WT mice. †$P < 0.05$; ††$P < 0.01$; †††$P < 0.001$ compared with vehicle-treated β-arrestin2$^{-/-}$ mice; significance was determined with one-way ANOVA with Bonferroni multiple comparisons post test.
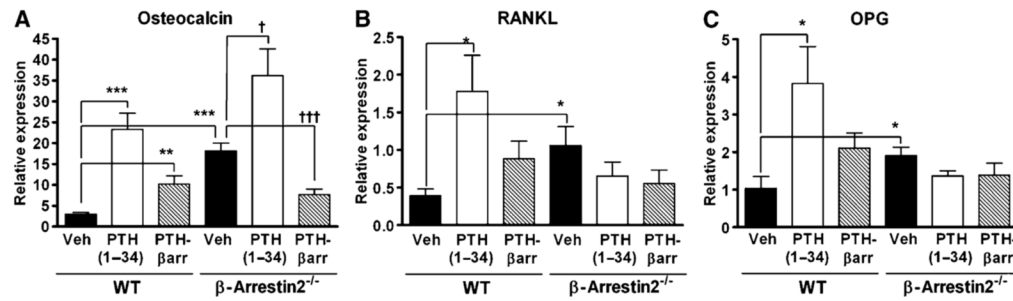
Fig. 6.
PTH-βarr induces β-arrestin–dependent expression of osteocalcin but not RANKL or OPG.
mRNA was isolated from the calvaria of male WT and β-arrestin2$^{-/-}$ mice treated with vehicle,
PTH(1–34), or PTH-βarr, and quantitative RT-PCR was used to determine relative gene
expression of protein modulators of bone metabolism: (**A**) osteocalcin, (**B**) RANKL, and (**C**)
OPG. Data represent the mean ± SEM from at least six mice. *$P < 0.05$; **$P < 0.01$; ***$P <
0.001$ compared with vehicle-treated WT mice. †$P < 0.05$; †††$P < 0.001$ compared with vehicle-
treated β-arrestin2$^{-/-}$ mice; significance was determined with one-way ANOVA with
Bonferroni multiple comparisons post test.